Comparison of the Response of a Simple Structure to Single Axis and Multiple Axis Random Vibration Inputs

Dan Gregory
Sandia National Laboratories
Albuquerque NM 87185 (505) 844-9743

Fernando Bitsie
Sandia National Laboratories
Albuquerque NM 87185 (505) 844-3182

David O. Smallwood
Consultant
9817 Pitt Pl. NE
Albuquerque NM 87111 (505) 296-2931

Random vibration experiments were performed on a simple structure to compare the response to single axis inputs and multiple axis inputs. The experiments were performed on a six degree of freedom (6-DOF) electrodynamic shaker described in a companion paper [1]. The simple structure consisted of a lumped mass mounted on the end of a short rectangular beam. A finite element analysis of the structure was also performed. The experimental and model results are discussed in the paper.

INTRODUCTION

Vibration environments that are realized in the true field environments are usually multi-dimensional and in the most general case are described by six degrees of freedom (three translations and three rotations). Due to the difficulties of generating and controlling multi-axis test environments, the development and qualification testing is usually performed with three single axis tests. The rotational accelerations are usually unknown and are ignored in the specification and constrained by the single axis tests to be small. This approach assumes that if the system or component survives the three single axis tests then it will survive in the full use environment which will likely have multi-axis excitations.

If the response of a structure is modeled as the superposition of the modal responses [2] then the instantaneous stress state realized in a structure is related to the number, amplitude, and phase relationships of the modes participating in the response. The number, amplitude, and phase relationships of the modes participating in the response are in turn related to the input forces (number, amplitudes, phases, locations, and directions) as well as the dynamics of the structure itself. It is anticipated that the response of a structure will be much different if simultaneously excited in multiple axes versus a single axis at a time. As the use of multi-axis shaker systems is becoming more common, researchers [3,4,5,6] are reporting more evidence of differences in failure modes and fatigue life for multi-axis loadings versus single axis inputs.

A simple structure was designed, fabricated, and tested utilizing a true six degree of freedom electrodynamic shaker system described in a companion paper [1]. Experiments were performed in single axes and multiple axes to compare the responses of the structure under the different loadings. A finite element model of the structure was also used to investigate the differences in the calculated Von Mises stress (magnitude and location).

DESCRIPTION OF SIMPLE TEST STRUCTURE

A simple structure was designed to provide several distinct vibration modes that would lie within a test bandwidth of 10 – 2000 Hz. The simple aluminum structure consisted of a lumped mass mounted on the end of a short rectangular beam. The beam is bolted to a plate shown in Figure 1. A finite element model was developed and the first six elastic modes are shown in Figure 2. Since the section of the beam was chosen to be rectangular, two distinct bending modes in each lateral direction were realized along with a torsional and axial mode. The model predicted frequencies ranged from 93 Hz for the first bending mode to 1552 Hz for the axial mode.

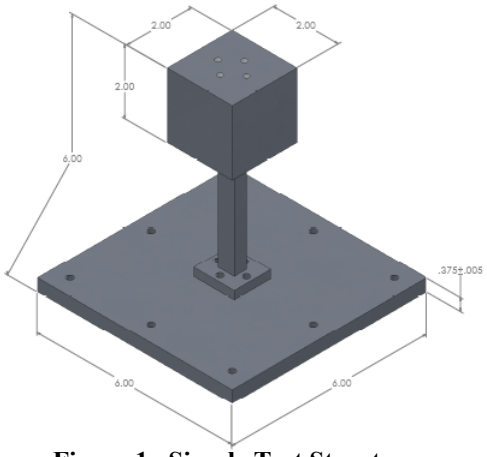

Figure 1. Simple Test Structure

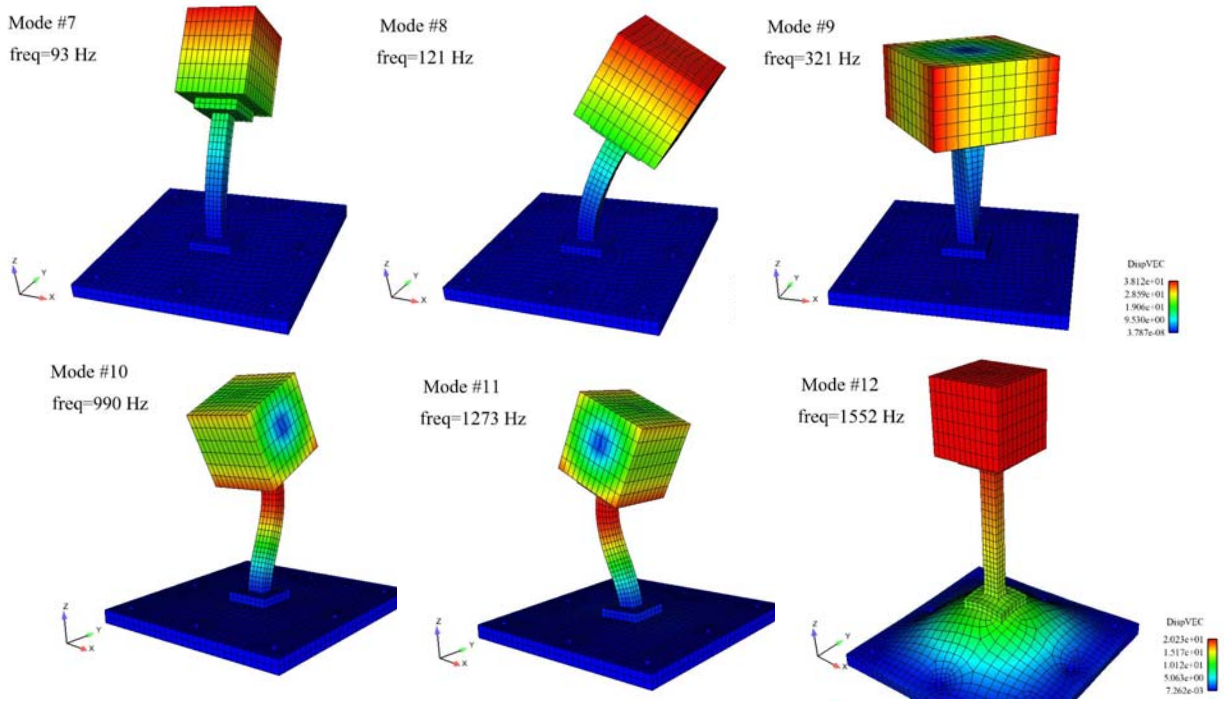

Figure 2. Mode Shapes and Frequencies

FINITE ELEMENT MODEL VON MISES STRESS RESULTS

The finite element model was used to calculate the maximum Von Mises stress magnitude and location with single axis and multiple axis loadings. The model was driven with a flat PSD at .001g^2/Hz over a bandwidth of 10 – 2000 Hz in each translation axis individually, and then with a two axis lateral input and finally a three axis input at the same input levels (uncorrelated). The results for the single axis loadings are shown in Figure 3 where the results for the lateral (X and Y) single axis loadings show the maximum Von Mises stress occurs along the outer fibers across the sections near the base as would be anticipated with the beam bending in a single direction. The axial (Z) loading shows a near uniform stress in the beam due to the inertial loading of the mass yielding an axial stress in the beam. The multi-axis loadings, however, show that the maximum Von Mises stress occurs at the corners of the beam due to the different bending behavior under the combined loadings. This analysis shows, as anticipated, that the maximum stress occurs at different locations for the combined axis loadings than for the single axis loadings.

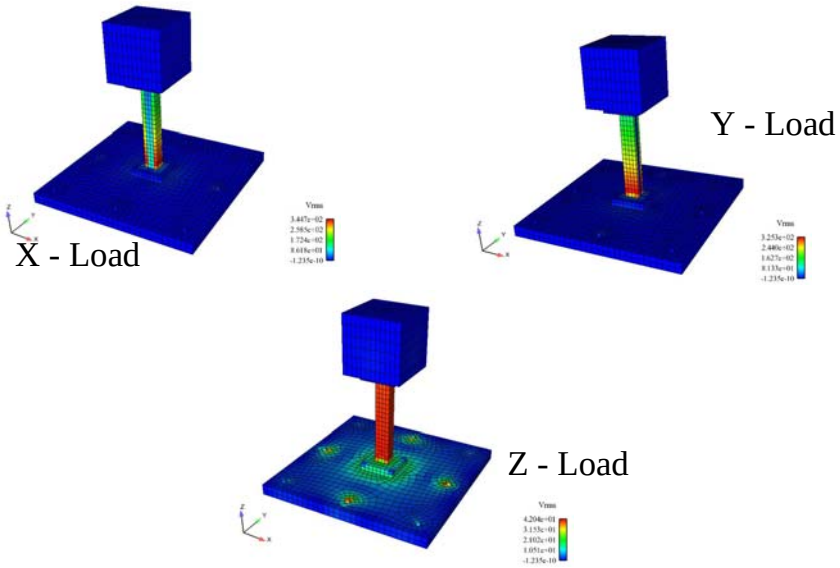

Figure 3. Maximum Von Mises Stress for Single Axis Inputs

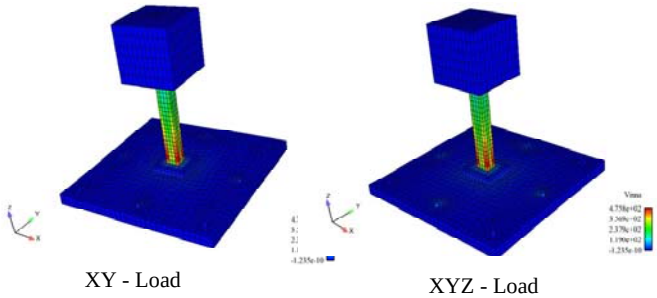

Figure 4. Maximum Von Mises Stress for Combined Axis Inputs

The calculated maximum Von Mises stress is listed in Table 1 for each input loading. The combined input results show significantly higher Von Mises stress than for the single axis inputs. Since the random vibration inputs to the linear model were uncorrelated, the stresses add as the square root of the sum of the squares of the single axis results. The results show that the maximum stress magnitude and the location are different for the combined axis loads versus the single axis loads.

Table 1. Maximum Von Mises Stress

Input Loading	Maximum Von Mises Stress (PSI)
X-Input	345
Y-Input	325
Z-Input	42
Combined XY- Input	474
Combined XYZ-Input	476

EXPERIMENTAL SETUP

A series of experiments were performed on the test structure with a true six degree-of-freedom (6-DOF) electrodynamic shaker system manufactured by Team Corporation (TE6-900) discussed in a companion paper [1]. The shaker system utilizes 12 electrodynamic shakers attached to a vibration table through hydraulic bearing assemblies. Four shakers provide inputs in each of the three orthogonal directions. By choosing the phase relationships between the shakers all six rigid body modes (three translations and three rotations) can be excited. Each of the 6-DOFs can be independently generated or superimposed in any desired combination.

The experimental setup on the 6-DOF shaker is shown in Figure 5. Triaxial accelerometers were mounted at several locations on the test structure and vibration table. Axial piezoelectric strain gages were also mounted on the four sides of the beam. The Spectral Dynamics Corporation Jaguar MIMO control system was used to control the 6-DOF shaker system. The Input/Output transformation option in the Jaguar system was used to define the input control degrees of freedom based on the four tri-axial accelerometers on the corners of the vibration table and to define the output mapping of the drives for the 12 shakers. The input transformation defines the X, Y, and Z translation DOFs as the average of the four X,Y, and Z-axis accelerometer channels on the table, respectively. The rotations about the X, Y, and Z (R_X, R_Y, R_Z) axes are computed by differencing the accelerometers and dividing by the distance between them. The input transformation was chosen to scale the rotations with unity length. The six outputs were transformed to twelve drive signals using another simple output transformation matrix, which allows all the terms in the matrix to be of comparable magnitude to assist the matrix inversion process. It was assumed that the accelerometers and shakers were well matched such that the transformation matrices were independent of frequency and could be deduced from rigid body considerations.

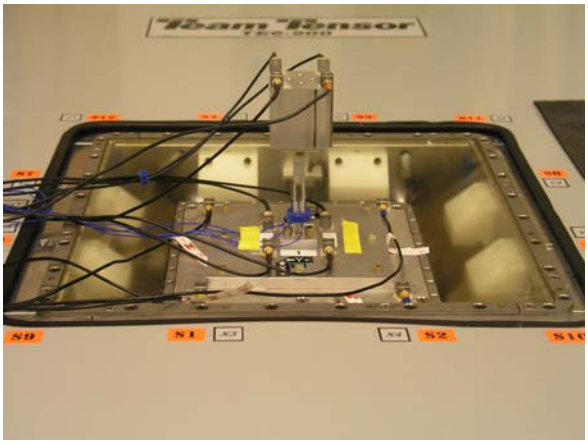

Figure 5. Experimental Setup on 6-DOF Shaker

The input transformation to define the control degrees of freedom in terms of the measured accelerations on the four corners of the vibration table is given by Eq. (1):

$$\begin{Bmatrix} X \\ Y \\ Z \\ R_X \\ R_Y \\ R_Z \end{Bmatrix} = \begin{bmatrix} .25 & .25 & .25 & .25 & 0 & 0 & 0 & 0 & 0 & 0 & 0 & 0 \\ 0 & 0 & 0 & 0 & .25 & .25 & .25 & .25 & 0 & 0 & 0 & 0 \\ 0 & 0 & 0 & 0 & 0 & 0 & 0 & 0 & .25 & .25 & .25 & .25 \\ 0 & 0 & 0 & 0 & 0 & 0 & 0 & 0 & .25 & -.25 & -.25 & .25 \\ 0 & 0 & 0 & 0 & 0 & 0 & 0 & 0 & .25 & .25 & -.25 & -.25 \\ -.125 & .125 & .125 & -.125 & -.125 & -.125 & .125 & .125 & 0 & 0 & 0 & 0 \end{bmatrix} \begin{Bmatrix} A1_X \\ A2_X \\ A3_x \\ A4_X \\ A1_Y \\ A2_Y \\ A3_Y \\ A4_Y \\ A1_Z \\ A2_Z \\ A3_Z \\ A4_Z \end{Bmatrix} \quad (1)$$

The output transformation for the drives to the twelve shakers from the computed drives for the control degrees of freedom is given by Eq. (2):

Drives to Shakers — Inverse of Output Transformation Matrix — Drives in Control Variable Coordinates

$$\begin{Bmatrix} D1_X \\ D2_X \\ D3_X \\ D4_X \\ D5_Y \\ D6_Y \\ D7_Y \\ D8_Y \\ D9_Z \\ D10_Z \\ D11_Z \\ D12_Z \end{Bmatrix} = \begin{bmatrix} .25 & .25 & -.25 & -.25 & 0 & 0 & 0 & 0 & 0 & 0 & 0 & 0 \\ 0 & 0 & 0 & 0 & .25 & .25 & -.25 & -.25 & 0 & 0 & 0 & 0 \\ 0 & 0 & 0 & 0 & 0 & 0 & 0 & 0 & .25 & .25 & .25 & .25 \\ 0 & 0 & 0 & 0 & 0 & 0 & 0 & 0 & .25 & -.25 & -.25 & .25 \\ 0 & 0 & 0 & 0 & 0 & 0 & 0 & 0 & .25 & .25 & -.25 & -.25 \\ -.125 & .125 & -.125 & .125 & -.125 & .125 & -.125 & .125 & 0 & 0 & 0 & 0 \end{bmatrix}^{-1} \begin{Bmatrix} X_{drive} \\ Y_{drive} \\ Z_{drive} \\ R_{X-drive} \\ R_{Y-drive} \\ R_{Z-drive} \end{Bmatrix} \quad (2)$$

EXPERIMENTAL RESULTS

The MIMO control system was configured for a full 6-DOF random vibration input from 20 – 2000 Hz with zero coherence between the inputs. The PSD level of 0.0032 g^2/Hz were chosen to yield an overall level of 2.5 grms for the X, Y, and Z translations and 15.5 $(rad/sec^2)^2$/Hz for and overall level of 175 rad/sec^2 for the R_X, R_Y, R_Z rotations. The shaker and control system simultaneously achieved the desired input levels for all DOFs as seen in Figures 6 and 7.

The system was then configured for single axis translational tests with the other degrees of freedom specified to be three decades lower than the test axis. The PSD levels were selected to be the same as for the previous 6-DOF test to allow comparison of responses for single axis vs. multi-axis inputs. A test was also performed with the three translations simultaneously applied and the rotations constrained to be small. The input control plots for the X-axis only testing are shown in Figures 8 and 9. As seen the control was very good for the input axis with some difficulty of constraining the other degrees of freedom at the frequencies of bending modes. This simple structure was lightly damped which provided a large dynamic range which challenges any shaker and control system to control (or constrain). Similar input control results were achieved for the other single translation axis and the simultaneous three translational axis tests.

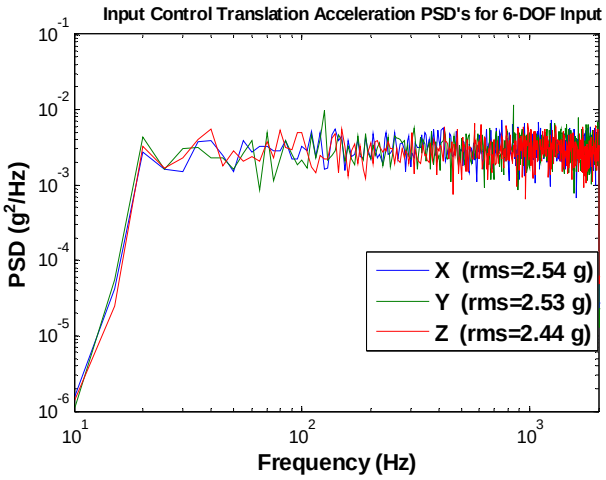

Figure 6. Input Control PSD's for the Translations for Full 6-DOF Input

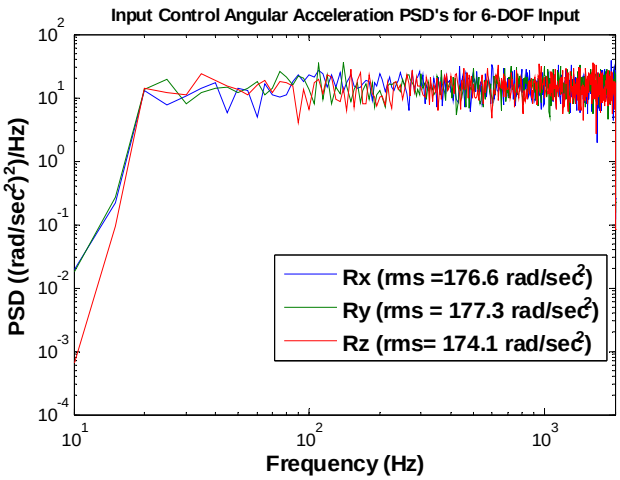

Figure 7. Input Control PSD's for the Rotations for Full 6-DOF Input

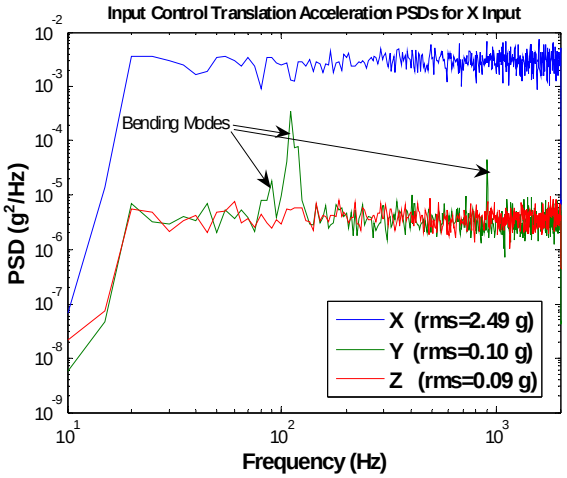

Figure 8. Input Control Translation PSD's for X-Input

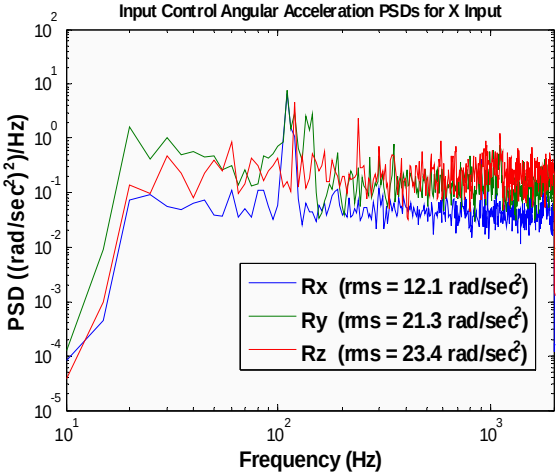

Figure 9. Input Control Angular Acceleration PSD's for X Input

The translations and rotations of the mass due to the different excitations were computed using a very similar linear transformation of the measured accelerations on the mass as were used for the accelerations measured on the base to define the control degrees of freedom. A comparison of the translation PSD's for the single X-axis input and the full 6-DOF input are shown in Figures 10 and 11. As anticipated, the translational response of the mass primarily occurs in the X-axis for the single X-axis input, but occurs simultaneously at substantial levels in all three translational directions for the 6-DOF excitation. Examining the rotations for the X-axis only input, the only rotational acceleration of significant amplitude occurs about the Y-axis (R_y) due to the bending response while significant rotational acceleration responses simultaneously occur about all three axes for the 6-DOF input. The comparison of the rotational PSD's for the single X-axis input and the full 6-DOF input are shown in Figures 12 and 13. The results for the different tests are summarized in Table 2 and 3 for the translational accelerations and rotational accelerations of the mass, respectively. Since the inputs are uncorrelated the instantaneous magnitude of the resultant acceleration vector can be estimated by computing the square root of the sum of the squares of the three

components. The direction of the resultant instantaneous acceleration vector will vary randomly due to the random phase relationships among the vector components. The combined axis tests generate significantly higher translation and angular accelerations than do the single axis tests.

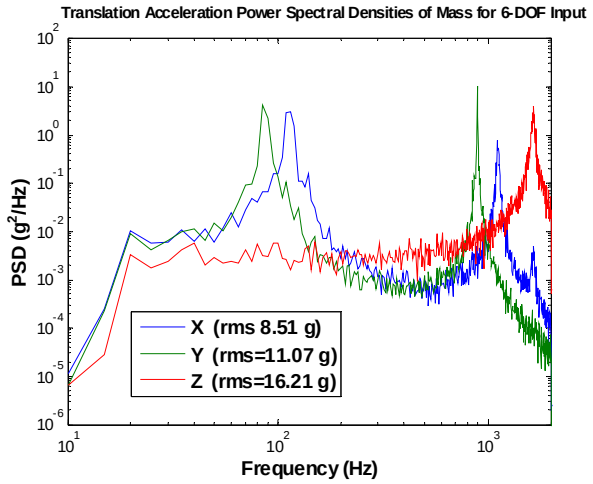

Figure 10. Translational Acceleration Response for the Full 6-DOF Input

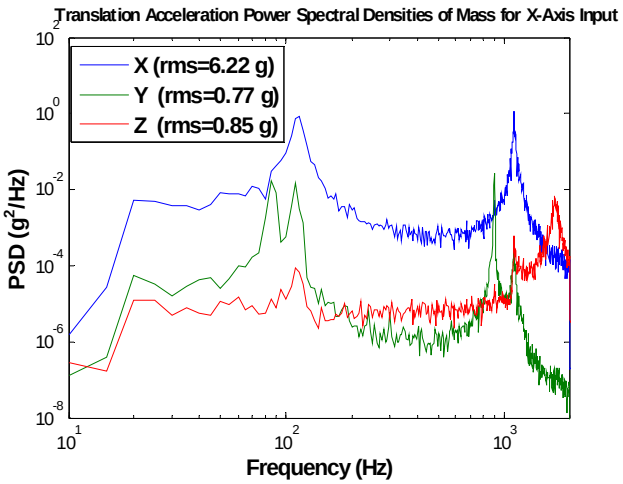

Figure 11. Translational Acceleration Response for the X-Axis Input

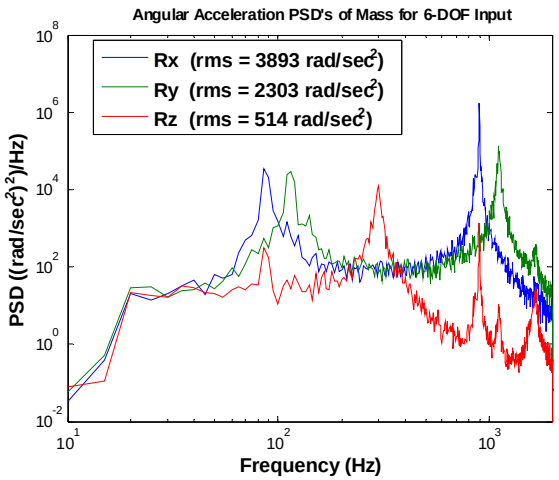

Figure 12. Angular Acceleration Response with the Full 6-DOF Input

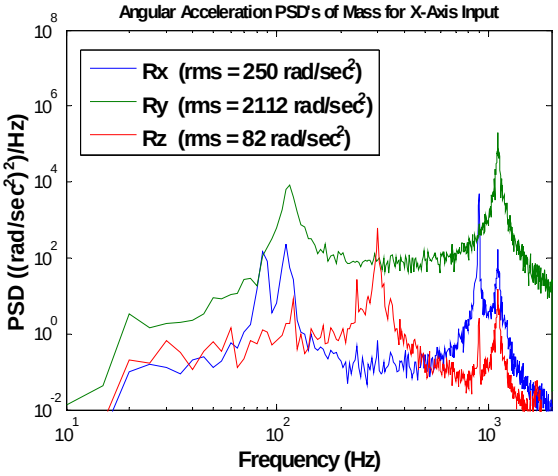

Figure 13. Angular Acceleration Response for the X-Axis Input

Axial strain measurements were also made on the four sides of the beam. These results for the 6-DOF input and the X-Axis input are shown in Figures 14 and 15. These strain gages are not sufficient to provide the principal stresses but do show that the axial strain levels are much higher on all sides of the beam than for the single axis input which primarily excites the bending in only one direction. Similar results were obtained for the other single axis input cases as shown in Table 4.

Table 2. Translational Accelerations of the Mass

Input	A_x RMS X-Axis (g)	A_y RMS Y-Axis (g)	A_z RMS Z-Axis (g)	$\sqrt{A_x^2 + A_y^2 + A_z^2}$ (g)
X	6.22	0.77	0.85	6.33
Y	0.63	9.46	0.63	9.50
Z	1.02	0.70	16.54	16.58
XYZ	6.67	11.28	15.48	20.28
6-DOF	8.51	11.07	16.21	21.40

Table 3. Angular Accelerations of the Mass

Input	R_x RMS X-Axis (rad/sec^2)	R_y RMS Y-Axis (rad/sec^2)	R_z RMS Z-Axis (rad/sec^2)	$\sqrt{R_x^2 + R_y^2 + R_z^2}$ (rad/sec^2)
X	6.22	0.77	0.85	6.33
Y	0.63	9.46	0.63	9.50
Z	1.02	0.70	16.54	16.58
XYZ	6.67	11.28	15.48	20.28
6-DOF	8.51	11.07	16.21	21.40

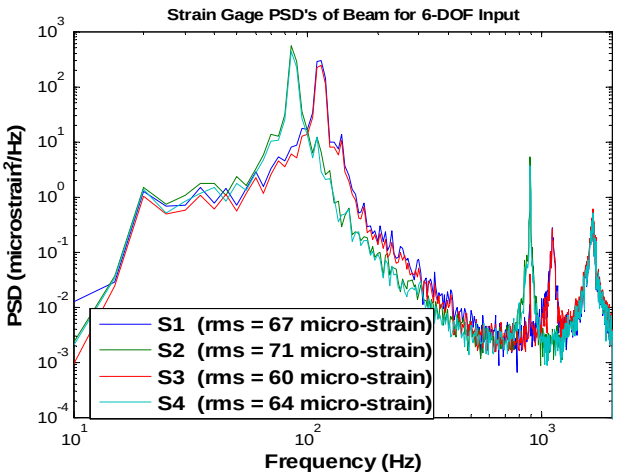

Figure 14. Strain Measurements for Full 6-DOF Input

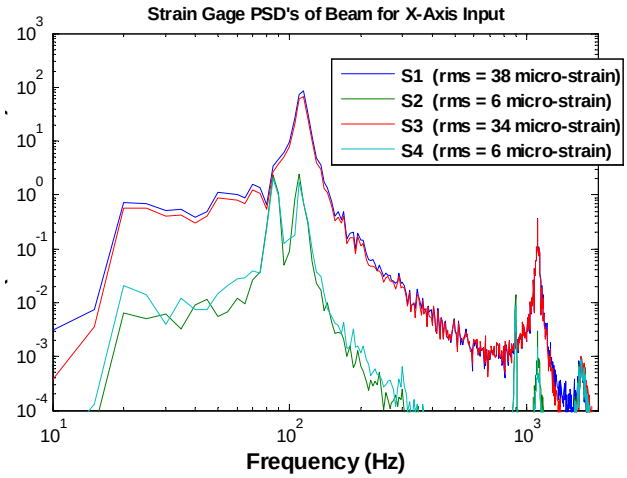

Figure 15. Strain Measurements for X-Axis Input

Table 4. Strain Measurements on Beam

Input	S_1 RMS Strain (μ-strain)	S_2 RMS Strain (μ-strain)	S_3 RMS Strain (μ-strain)	S_4 (μ-strain)
X	6.22	0.77	0.85	6.33
Y	0.63	9.46	0.63	9.50
Z	1.02	0.70	16.54	16.58
XYZ	6.67	11.28	15.48	20.28
6-DOF	8.51	11.07	16.21	21.40

CONCLUSIONS

Experiments and analysis were performed on a simple structure to evaluate the response to single axis and multi-axis inputs. The analytical results show that the maximum Von Mises stress and the location were different for the combined axis loads versus the single axis loads. A 6-DOF electrodynamic shaker system was successfully used to perform single axis and multi-axis inputs including a full 6-DOF environment. The experimental results show significant differences in the acceleration response of the mass as well as the strain measured in the beam. These results demonstrate that the modal participations are different for the multi-axis tests and the resulting instantaneous stress and acceleration states are different, not only in magnitude, but also in location and direction. This indicates that the potential failure modes will be different. These results further reinforce the need to perform more realistic tests that include the simultaneous application of all translations and rotations inherent in the true vibration environment.

FUTURE WORK

The 6-DOF electrodynamic shaker system shows great promise for future investigations of combined axis testing and evaluating the inclusion of the rotations in the test environments. To date only uncorrelated inputs have been investigated and the specification and control with correlated inputs will be explored in the future.

REFERENCES

1. Smallwood, D.O. and Gregory, D.L. " Evaluation of a 6-DOF Electrodynamic Shaker System," Proceedings of the 79th Shock and Vibration Symposium, Orlando, FL., 2008.
2. Craig, R.R, 1981, *Structural Dynamics*, John Wiley & Sons, New York.
3. Berman, M.B. “Inadequacies in Uniaxial Stress Screen Vibration Testing.” *Journal of the IEST*, Vol. 44, No. 4, Fall 2001, pp. 20-30.
4. Freeman, M.T. “3-axis Vibration Test System Simulates Real World” Test Engineering and Management. Dec/Jan 1990-91, pp. 10-14.
5. Himelblau, H. and Hine, M.J. “Effects of Triaxial and Uniaxial Random Excitation on the Vibration Response and Fatigue Damage of Typical Spacecraft Hardware”. Proceedings of the 66th Shock and Vibration Symposium, Arlington, VA, 1995.
6. French, R.M., Handy, R., and Cooper, H L. “Comparison of Simultaneous and Sequential Single Axis Durability Testing”, Experimental Techniques, Vol. 30, No. 5, September/October, 2006, pp. 32-37.